Int. J. Heat Mass Transfer. Vol. 17, pp. 477 484. Pergamon Press 1974. Printed in Great Britain

FREE CONVECTION HEAT AND MASS TRANSFER UNDER CONDITIONS OF FROST DEPOSITION

LAWRENCE A. KENNEDY and JACK GOODMAN*
Faculty of Engineering and Applied Sciences, State University of New York at Buffalo, Buffalo, New York 14214, U.S.A.

(*Received* 4 *September* 1973)

Abstract—Frost formation on a vertical surface is investigated under natural convection conditions. Local heat and mass transfer coefficients from humid air to the frost surface are obtained, along with effective thermal conductivity and density of the frost.

A Mach–Zehnder interferometer is used to determine the temperature distribution in the boundary layer adjacent to the frost surface, thus allowing local values of the heat flux to be calculated. Observations of the frost structure are performed.

NOMENCLATURE

D, binary diffusion coefficient;
Gr_x, local Grashof number $= g\beta(T - T_\infty)x^3/\nu^2$;
g, acceleration due to gravity;
H, thickness of copper plate;
h, heat transfer coefficient;
h_D, mass transfer coefficient;
k, thermal conductivity;
k_f, effective thermal conductivity of frost;
L, latent heat of sublimation;
$\dot{m}_1$, mass flux of water vapor;
Nu_x, local Nusselt number $= hx/k$;
P, total pressure;
Pr, Prandtl number;
q_T, total heat flux;
S, thickness of frost layer;
T, temperature;
W, mass fraction;
y, coordinate normal to vertical surface.

Greek symbols

ρ, density;
σ, Stefan–Boltzmann constant;
ε, frost surface emissivity.

Subscripts

i, i'th species component (1 = water vapor, 2 = dry air);
0, frost surface–air interface;
∞, ambient;
cu, copper;
f, frost;
w, wall (copper surface);
a, alcohol.

1. INTRODUCTION

THE PHENOMENA of frost formation is encountered in a variety of applications which involve surfaces at low temperatures. If the surface is maintained below both the dew point and the freezing point of the condensible species in a gas, this species will condense in the form of a solid deposit. The problem studied herein examines this phenomena for water vapor in air. Typically, the thickness of the deposited frost layer will increase with time while the heat transfer decreases. This process is governed by energy and mass transport across the boundary layer. The physical process is shown in Fig. 1.

The bulk of studies connected with this phenomena have been directed towards forced convection and a review of such work is presented in [1] and [2]. Reports of studies on the heat and mass transfer under frosting conditions in natural convection, however, is extremely limited. Whitehurst [3] first examined natural free convection frost deposition, measuring the frost surface temperature and boundary layer temperature profile with thermocouples. He obtained qualitative agreement between his experimental and predicted boundary layer temperatures. Barron and Han [4] investigated a similar problem for a cryogenically cooled plate, obtaining correlations for the heat and mass transfer coefficients. However, in their study, "fog" was formed in the boundary layer due to the cryogenic temperatures employed and their experimental data varied from 10 per cent to an order of magnitude below their predictions.

*Presently at Faculty of Mechanical Engineering, Technion—Israel Institute of Technology, Haifa, Israel.

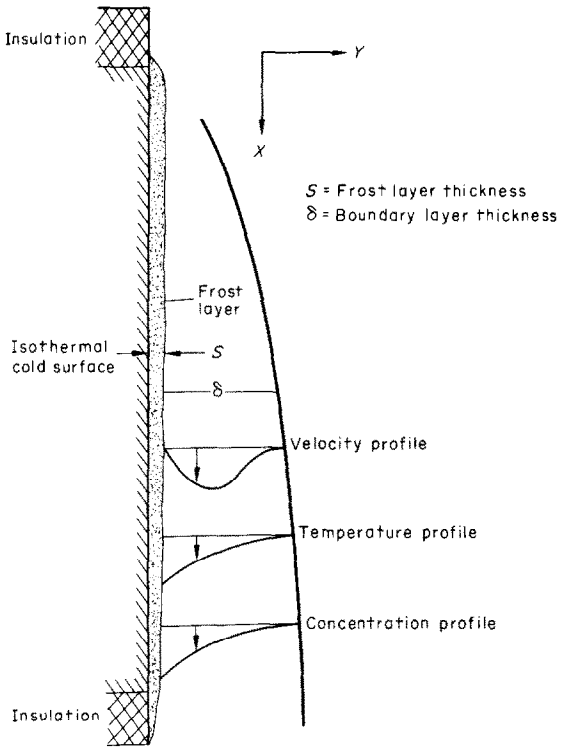

FIG. 1. Model of the free convection boundary layer adjacent to a frost layer.

In a more recent work, Goodman and Kennedy [5] examined a similar problem with the vertical surface cooled by cold alcohol and the boundary layer temperatures determined interferometrically. Their analysis showed the overall frosting process to consist of a moving boundary problem coupled to an adjacent free convection boundary layer problem. However, due to the different time scales associated with the conduction and convection processes, it was shown that the free convection boundary layer problem could be solved independently of the moving frost surface problem and only serves as a boundary condition to it. Good agreement was obtained between the heat transfer and mass flux predicted by this approximation and those measured. The main difficulty in making heat transfer and mass flux predictions lies in the small amount of information available on the thermal conductivity, density, and the coefficients of heat and mass transfer for frost.

Thermal conductivity and density data for frost forming on a horizontal surface placed in a wind tunnel was obtained by Biguria [2]. He found that the frost density varied with distance approximately as the heat transfer coefficient varied, and that the frost thickness appeared to be independent of position. Average values for the frost thermal conductivity were obtained from an overall heat balance on the system. In their earlier work, Goodman and Kennedy [5] reported the results of some preliminary measurements on frost thermal conductivity and heat transfer coefficients for free convection.

In this paper, further experimental results are reported on the heat and mass transfer coefficients, thermal conductivity, and density of frost. These results were obtained for the frosting of a cold surface with an adjacent natural convection boundary layer.

II. EXPERIMENTAL APPARATUS

The experimental equipment used in these studies is similar to that previously described by Goodman and Kennedy [5]. It consists of a vertical constant temperature surface with associated cooling apparatus, a Mach–Zehnder interferometer with 15 cm dia mirrors, a Mettler side loading balance, a low power microscope with micrometic stage, and instrumentation to measure ambient temperature and humidity.

The entire apparatus and optical system was placed in a room with a volume of approximately 250 m^3 where the relative humidity could be regulated over the range 30–80 per cent at about 24°C. In this study, two different copper surfaces were employed: one had a large radius of curvature and a second flat plate had small surface segments which could be removed. The former was principally used for heat transfer measurements and the latter for frost density measurements. Both plates were orientated in the vertical direction.

Considerations of the number of fringe shifts required for good accuracy on the interferograms dictated a radius of curvature greater than 50 cm, with the temperature differences used here. The exact radius of curvature was not critical and the surface was formed having a radius of curvature of 62·41 cm. This large radius of curvature very nearly approximated a flat plate, and more importantly allowed the interferometric data to be free of end effect errors which arise in a planar geometry. The boundary layer in this geometry is axisymmetric and the fringe shift-density relationship is described by an Abel integral. This integral is easily inverted and numerically calculated by the method of [6].

Using the curved surface, a number of experiments were performed with the plate both heated and cooled and the measured temperature distributions were found to lie on the flat plate similarity solution curve [11]. When the surface was cooled below 0°C, frost was observed to form uniformly over the entire area of the plate. Both vertical surfaces were made of copper and formed one side of insulated steel tanks. The insulation used on the tanks was closed-cell polyurethane foam, 2·5 cm thick.

Ethyl alcohol was used as a coolant and was pumped through the tanks via two inlets and one outlet. The coolant ports were arranged to promote sufficient fluid mixing so as to produce a uniform coolant temperature in the tank. The alcohol is cooled to the desired temperature by a Poly-Science Corp. Model KR30 Immersion Cooler and is circulated through the tank by a Haake Model FS Constant Temperature Circulator. Temperatures could be maintained down to $-17°C$ with an accuracy of $\pm 0{\cdot}5°C$ with a period of several hours. All lines between the cooler, circulator, and test tank were insulated so that a total heat balance could be done. The uniformity of the curved plate temperature was measured by eleven copper–constantan thermocouples imbedded halfway through the back of the 3·2 mm thick copper surface and arranged in a crossed array. During the tests, the plate temperature was uniform within $\pm 0{\cdot}2°C$. A similar thermocouple placed about 50 cm from the tank measured the ambient temperature. The ambient temperature was steady within the same limit as the coolant temperature. The thermocouple leads went to a Honeywell thermocouple rotary selector switch which was connected to a Leeds and Northrup Model 8686 millivolt potentiometer. The reference junction was a water–ice bath at 0°C, and the accuracy of the thermocouples corresponding to the smallest division on the potentiometer scale is close to 0·06°C.

The ambient humidity was monitored by a Lufft relative humidity gage. In all experimental runs, the level of the ambient relative humidity was maintained within 2 per cent. The copper test surface was placed in the test area of the interferometer and the interferograms were photographically recorded. Representative fringe shifts are shown in Fig. 2.

In addition to measuring the fringe shifts, the frost growth rates could be obtained from direct measurements of the photographs by measuring the distance from the frost surface to a reference point in space. Independent measurements of the frost thickness were also performed by viewing the surface through an alternate optical path. A telescope mounted on a micrometer track was used to measure the distance of the telescope cross hairs had to be traversed in order to line up with the frost surface. Results of both methods of measurement were in very close agreement.

The recording media used for the interference pictures is Kodalith Ortho Type 3 negative sheet film. As the speed of this high contrast film is very slow, exposure times of 15 s were required, but even for

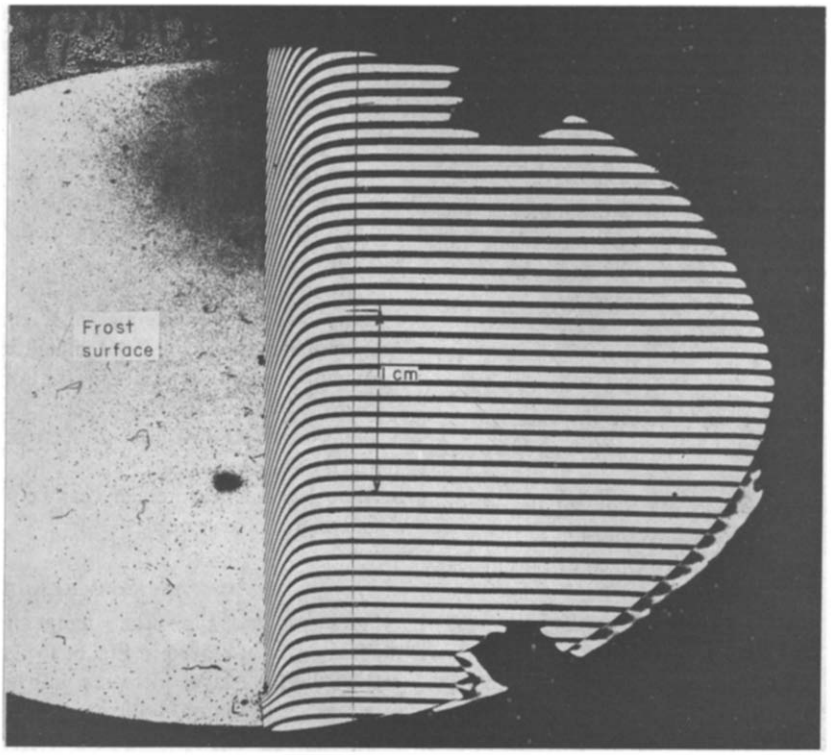

FIG. 2. Interferogram of fringe shift adjacent to frost surface $T_\infty = 22°C$, $T_w = -13°C$, $T_0 = 0°C$.

this long time, the pictures were never blurred, thus helping to show the quasi-steady nature of the boundary layer flow. All measurements were made directly on the negatives by a Nuclear Research Instruments Co. Measuring Projector. This device is normally used to plot bubble chamber particle tracks and has an accuracy in linear measurements of 0·005 mm. The combination of the high measurement resolution of this device and the unusually high contrast of the recording film allowed measurements to be made down to 1/50 of a fringe shift. Measurements of the frost density were performed on the planar plate with removable segments. At various distances from the plate's leading edge, removable segments of copper were machined to fit flush with the flat surface. The mass of each removable segment plus the frost layer on it was determined by a Mettler balance having an accuracy of 0·01 mg. The thickness of the frost layer was determined by using a low power microscope with micrometer stage to measure the total thickness of frost layer and segment and subtracting the thickness of the segment. These measurements were carried out under conditions of wall and ambient temperatures corresponding to those of the heat transfer measurements.

Inherent in these density measurements is an error associated with the actual volume of the frost being measured. When the surface segments are removed, the frost does not separate sharply, and consequently, the surface area of the segment is not always the same of the frost sample. However, by performing repeated tests, these errors in frost volume are minimized.

III. PRINCIPLES OF MEASUREMENT

The effective thermal conductivity of the frost layer, k_f, may be obtained at various positions along the surface by performing any energy balance across the copper surface and frost layer. This yields:

$$k_f = k_{cu}\frac{S}{H}\frac{(T_w - T_a)}{(T_0 - T_w)}. \tag{1}$$

Here H and S are, respectively, the thickness of the copper plate and frost layer at the axis point of measurement.

The total heat flux between the ambient air and the frost surface may be expressed as the sum of the conduction, phase change, and radiation contributions, i.e.

$$q_T = -k\frac{\partial T}{\partial y_0} + \dot{m}_1 L + \varepsilon\sigma(T_0^4 - T_\infty^4). \tag{2}$$

Additional energy transfer due to the Dufour effect can be shown to be negligible [4]. Since no liquid water was observed to form in these experiments, the latent heat of sublimation of water vapor rather than vaporization was used in the above calculations. In the radiation term, the emissivity of frost was taken as 0·985 [2, 7]. Once equation (2) is evaluated the local heat transfer coefficient, h, may be obtained from

$$q_T = h(T_0 - T_\infty). \tag{3}$$

The mass flux of water vapor to the frost surface is expressed by

$$\dot{m}_1 = \left[1 + \frac{W_0}{1 - W_0}\right]\rho D \left.\frac{\partial W}{\partial y}\right|_0. \tag{4}$$

The mass concentration gradient may also be determined simultaneously with the temperature by using two-wavelength interferometry. Unfortunately, this method proved to be unsatisfactory because of the low water vapor concentrations involved and the small wavelength dependence of the Gladstone–Dale constants of dry air and water vapor. Therefore, it was decided to determine an overall mass transfer coefficient, h_D, by making direct measurements of growth rates and density to obtain $\dot{m}_1$.

Once the mass flux of water vapor to the frost surface was obtained by this approach, the mass transfer coefficient was then calculated from

$$\dot{m}_1 = \rho h_D(W_0 - W_\infty) \tag{5}$$

where $W = 0{\cdot}662 \times \mathrm{RH} \times P_{sat}/P$. RH is the relative humidity, and P_{sat} is the saturation pressure. The relative humidity at the frost surface was taken to be 100 per cent with the saturation pressure of water vapor obtained from [2] as

$$\frac{P_{sat}}{P} = \exp[17{\cdot}3274 - 6134{\cdot}2865/T_0].$$

From the foregoing, the thermal conductivity, effective heat transfer coefficient, mass transfer coefficient, and density of the frost can be obtained if the following variables are measured:

(1) frost–air interfacial temperature;
(2) frost–copper surface interfacial temperature;
(3) ambient air and coolant temperatures;
(4) temperature distribution in the boundary layer;
(5) growth rate of the frost layer;
(6) mass of a given volume of the frost layer.

With the apparatus and procedures described in Section II, these measurements can be performed with a high degree of accuracy.

IV. DISCUSSION OF RESULTS

Some results of the surface temperature change of the frost layer are given in Fig. 3. Typically the thickness of the frost layer increases with time and tends to act as an insulator. Compared with the period of time involved in the frosting process, the time required for the frost surface temperature to approach 0°C is relatively fast. As the ambient humidity becomes larger,

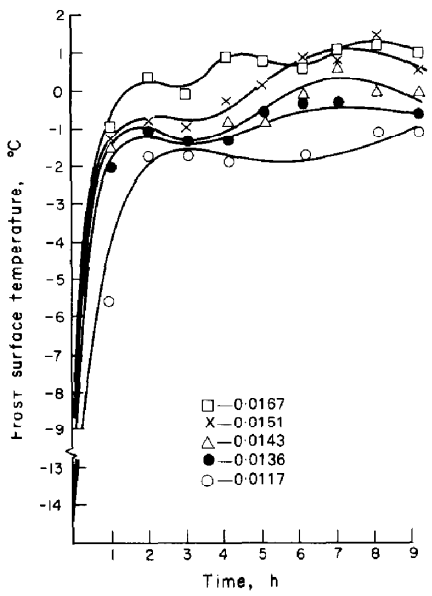

FIG. 3. Oscillation of the frost surface temperature at a position 130 mm from the leading edge.

this time decreases because of the greater amount of water vapor available to be deposited on the surface, and the subsequent more rapid growth rate of the frost surface. For all practical importance, the frost surface temperature increases within two degrees of 0°C within 1 h for specific humidities greater than 0·0136, and for smaller values of specific humidities within 2 h. One interesting feature of the temperature data is the unmistakable temperature oscillations of the frost surface around 0°C. This is shown over a time scale of 9 h in Fig. 3. Except at the very low specific humidities (0·017) where this cyclic temperature was observed having a period of 4–6 h. As the ambient humidity increased, the period of these oscillations was shortened. Close examination of the frost layer showed a definite pattern of change in its structure. Under the microscope, sublayers of more and less dense frost could be observed which are attributed to the cycling surface temperature. A similar observation was made by Smith [9] in his study of frost on cyrogenically cooled surfaces. In the present study, time periods up to 12 h were examined with this cyclic temperature observed in all cases.

The influence of humidity on the growth of the frost layer is shown in Fig. 4. After the initial period of frost build-up (0–3 h) during which time the frost surface temperature approaches 0°C, the thickness of the frost layer increases as a linear function of time. This linear growth rate was also observed in other investigations [10, 11]. As to be expected, a higher ambient humidity produces a thicker frost deposit, but the effect is mostly concentrated within the initial growth period. After this time period, the frost layer growth rate is only slightly greater (about 15 per cent) at the highest humidity than at the lowest. Water vapor diffusion and subsequent frost densification must account for this small increase since there is about 50 per cent more ambient water vapor available at the highest humidity than at the lowest. The frost deposition rates measured in the initial growth period were up to four times larger than those in the linear growth regime.

During the initial growth period, the convective heat flux decreased significantly and subsequently approached a constant value in the linear growth regime. Both the constant heat flux and growth rate are consistant in that both depend on the frost surface temperature which essentially approaches a constant value after 3 h.

As pointed out earlier, after the initial growth period, the frost surface temperature oscillates slightly about 0°C. However, because of the small magnitude of the temperature variation, the heat transfer may be correlated (Fig. 5) by the relation:

$$Nu_x = 0{\cdot}3733\, Gr_x^{1/4}.$$

The agreement for the coefficient on the right hand side is within 5 per cent of the results obtained from a similarity solution [11] for a Prandtl number of 0·72.

The change with time of the effective heat and mass transfer coefficients are shown in Figs. 6 and 7. Both slightly increase with time. Initially this was believed to be contradictory to the measured heat flux data which decreases to a constant value with time due to the insulation effect of the frost on the cold surface. However, due to the porosity of the frost layer, the effective surface area becomes larger than just the projected surface area of the cold surface as the frost layer

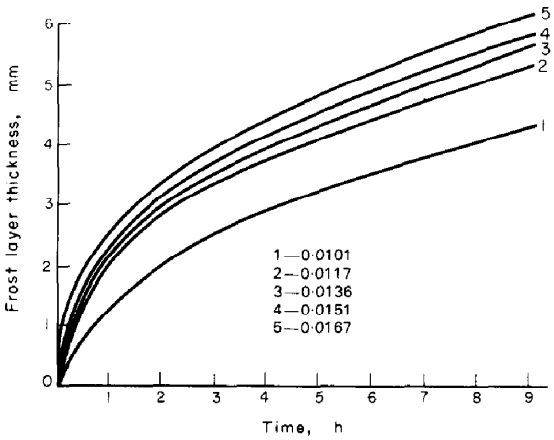

FIG. 4. Influence of humidity on the frost growth at a position 130 mm from the leading edge.

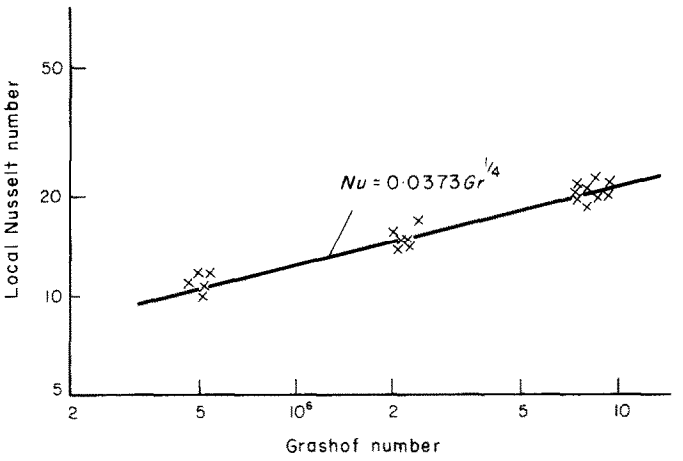

FIG. 5. Local Nusselt number as a function of Grashof number.

grows with time. Since the actual area of heat transfer increases with time, the apparent heat transfer coefficient must also increase. Similar arguments can be made for the mass transfer coefficient.

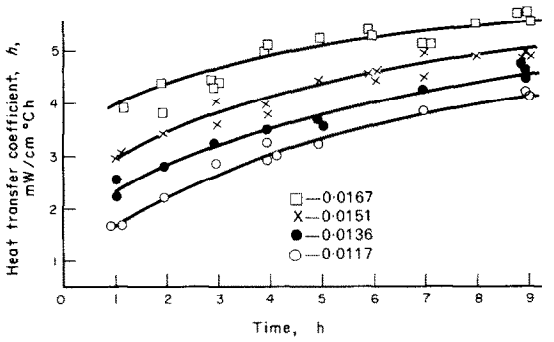

FIG. 6. Variation of the heat transfer coefficient with time and humidity.

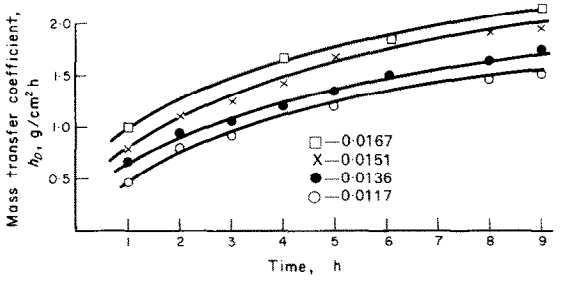

FIG. 7. Variation of the mass transfer coefficient with time and humidity.

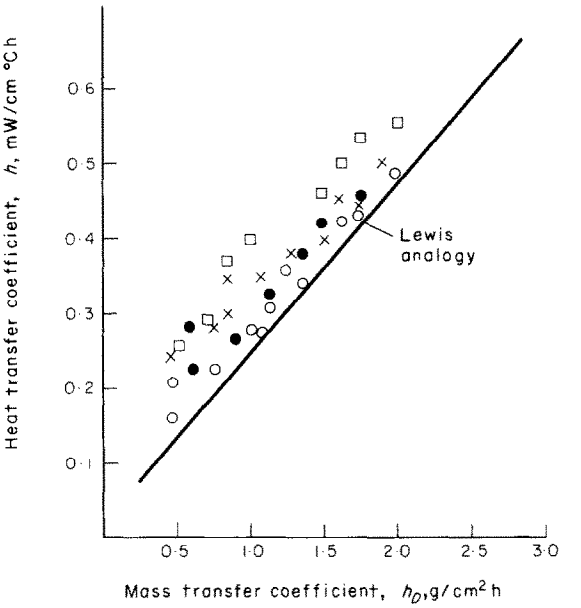

FIG. 8. Correlation between heat transfer and mass transfer coefficients.

The heat and mass transfer coefficients are cross plotted in Fig. 8. It is seen that while an analogy between h and h_D exists, it lies above the Lewis analogy. The same result was observed by Yamakawa *et al.* [12] in a study of frost formation under forced convection conditions.

The frost weight per unit surface area is shown in Fig. 9 for different humidities. It may be observed that this weight per unit surface area is also approximately linearly proportional to time, and a higher ambient humidity produces a heavier frost deposit.

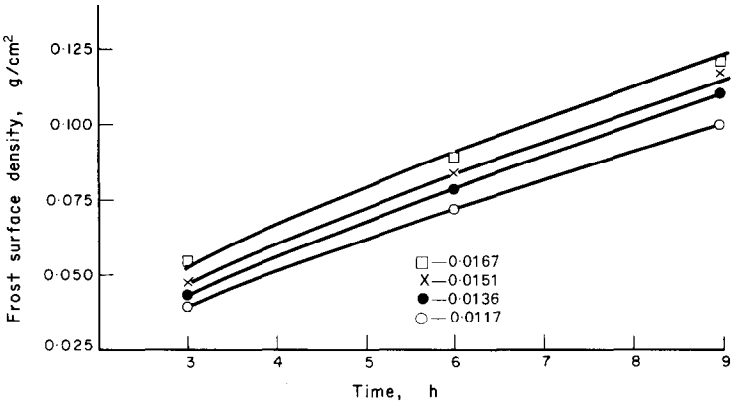

FIG. 9. Frost surface density variation with time and humidity at a position of 130 mm from the leading edge.

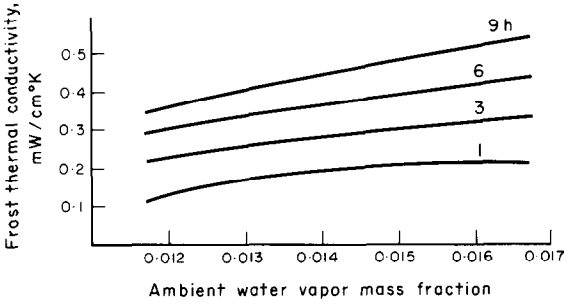

FIG. 10. Frost thermal conductivity as a function of the ambient water vapor mass fraction at 130 mm from the leading edge.

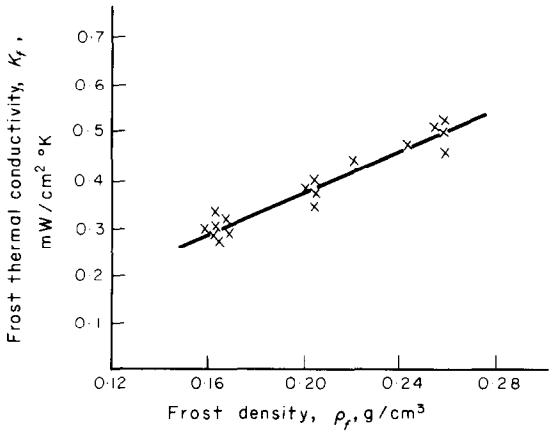

FIG. 11. Thermal conductivity as a function of the frost density.

Since frost has a porous structure, conduction within the frost layer is inhibited due to its large air void fraction and the internal frost energy transfer must be strongly influenced by water vapor diffusing from the air–frost interface into the colder frost layer. This internal diffusion of water vapor causes the frost layer to become more dense and thus the thermal conductivity is a function of time. As seen in Fig. 10, the thermal conductivity slightly increases with the ambient humidity and continues to increase with time (frost thickness).

The density of the frost layer was measured, and found to be an approximate linearly increasing function of time and thus showed that the frost layer densified with time. In Fig. 11 the thermal conductivity increases with increasing frost density in agreement with our earlier discussion. Over the range of these measurements, the thermal conductivity and density could be linearly related.

CONCLUSIONS

The principal results obtained in this study are:

(1) Cyclic surface temperatures ($\pm 1\frac{1}{2}$°C) of the frost were recorded and cyclic density variation observed as the frost layer grew with time.

(2) As a result of measurements of the frost surface weight and thickness, it must be concluded that in addition to deposition at the frost–air interface, appreciable frost is formed within the porous layer.

(3) The convective heat transfer decreases with time during the initial growth of the frost deposit, and subsequently approaches a constant value.

(4) The effective heat transfer and mass transfer surface area is increased due to the porous structure

of the frost layer. This causes the apparent heat and mass transfer coefficients to increase with time. The correlation between these two coefficients is greater than that predicted by the Lewis analogy.

(5) The frost density increases with time and influences the effective thermal conductivity. For the range of these experiments, k_f and ρ_f are linearly related.

REFERENCES

1. J. Goodman, Free convection frost formation on cool surfaces, Ph.D. Dissertation, State University of New York at Buffalo (1972).
2. G. O. Biguria, The moving boundary problem with frost deposition to a flat plate at subfreezing temperatures and forced convection conditions. The measurement and correlation of H_2O frost properties, Ph.D. Dissertation, Lehigh University (1968).
3. C. H. Whitehurst, Heat and mass transfer to a metal plate, *ASHRAE Jl* **4**, 104–116 (1962).
4. R. F. Barron and L. S. Han, Heat and mass transfer to a cryo-surface in free convection, *J. Heat Transfer* **87C**, 499–506 (1965).
5. J. Goodman and L. A. Kennedy, Free convection frost formation on cool surfaces, *Proceedings of the 1972 Heat Transfer and Fluid Mechanics Institute*, pp. 338–352. Stanford University Press.
6. O. H. Nestor and H. N. Olsen, Numerical methods for reducing line and surface probe data, *SIAM Rev.* **2**, 200–207 (1960).
7. N. E. Dorsey, *Properties of Ordinary Water Substances*. Reinhold, New York (1940).
8. R. V. Smith, K. D. Edmonds, E. G. F. Brentari and R. J. Richards, Analysis of frost formation on a cryosurface, *Advances in Cryogenic Engineering*, Vol. 9, p. 88. Plenum Press, New York (1963).
9. J. L. Loper, Frost formation upon a thin aluminum tank containing liquid oxygen, *ASHRAE Trans.* **66**, 104 (1960).
10. F. E. Ruccia and C. M. Mohr, Atmospheric heat transfer to vertical tanks filled with liquid oxygen, *Advances in Cryogenic Engineering*, pp. 307–318. Plenum Press, New York (1960).
11. S. Ostrach, An analysis of laminar free convection flow and heat transfer about a flat plate parallel to the direction of the generating body forces, NACA TR-1111 (1953).
12. N. Yamakawa, N. Takahash and S. Ohtani, Forced convection heat and mass transfer under frost conditions, *Heat Transfer—Japan. Res.* **1**(2), 1–10 (April-June 1972).

TRANSFERT DE MASSE ET DE CHALEUR PAR CONVECTION NATURELLE SOUS DES CONDITIONS DE GIVRAGE

Résumé—On étudie la formation de givre sur une surface verticale dans des conditions de convection naturelle. Les coefficients locaux de transfert de chaleur et de masse entre l'air humide et une surface givrée sont obtenus en fonction de la conductivité thermique effective et de la densité du givre.

On a utilisé un interféromètre de Mach-Zehnder pour déterminer la distribution de température dans la couche limite adjacente à la surface givrée, permettant ainsi le calcul des valeurs locales du flux thermique. On a aussi observé la structure du givre.

HMT No. 469

WÄRME- UND STOFFÜBERTRAGUNG BEI FREIER KONVEKTION UND REIFABLAGERUNG

Zusammenfassung—Die Reifbildung an einer senkrechten Oberfläche wird unter den Bedingungen der freien Konvektion untersucht. Örtliche Wärme- und Stoffübergangskoeffizienten von feuchter Luft an die Reifoberfläche werden, gleichzeitig mit der effektiven Wärmeleitfähigkeit und der Reifdichte, ermittelt.

Zur Bestimmung der Temperaturverteilung in der Grenzschicht längs der Frostoberfläche wird ein Mach-Zehnder-Interferometer benutzt. Diese Methode erlaubt die Berechnung örtlicher Wärmestromdichten. Beobachtungen der Reifstruktur wurden durchgeführt.

ТЕПЛО- И МАССООБМЕН ПРИ СВОБОДНОЙ КОНВЕКЦИИ В УСЛОВИЯХ ОБРАЗОВАНИЯ ИНЕЯ

Аннотация — Исследуется образование инея на вертикальной поверхности при естественной конвекции. Получены локальные коэффициенты тепло- и массообмена влажного воздуха с поверхностью инея, а также эффективные коэффициенты теплопроводности и значения плотности инея.

Для нахождения распределения температуры в пограничном слое на поверхности инея использовался интерферометр Маха-Цендера, что позволило рассчитать локальные значения теплового потока. Исследовалась структура инея.